Nix, A. R., Anderson, H. R., & McGeehan, J. P. (1993). Estimating wideband bit error rates using pilot tone envelope fading statistics. 577 - 582.

Link to publication record in Explore Bristol Research

PDF-document

University of Bristol - Explore Bristol Research

General rights

Estimating Wideband Bit Error Rates Using Pilot Tone Envelope Fading Statistics

A.R. Nix, H.R. Anderson[1] & J.P. McGeehan

Centre for Communications Research, University of Bristol,
Queen's Building, University Walk, Bristol, United Kingdom, BS8 1TR
Tel: +44 272 303727   Fax: +44 272 255265

Abstract

In this paper a number of techniques are investigated for predicting the performance of a digital system in fading channels. A method is presented which combines both bit error rate simulation and site-specific channel characterisation using ray tracing techniques. Probability density functions are developed for the resulting signal variations which show instantaneous bit error rate versus fade depth. Using this approach, the irreducible error rate for both random FM and RMS delay spread have been determined for π/4 DQPSK. It is shown that RMS delay spread alone cannot fully represent the distorting effect of the wideband channel. However, if combined with narrowband fading statistics, it becomes possible to estimate the average bit error rate for a given propagation environment. To increase the speed of our fading simulations, an importance sampling approach has also been developed which yields results that are comparable to those generated from full simulations.

I - INTRODUCTION

Future mobile systems are now looking towards the integration of voice with high capacity data based services. However, unlike the majority of analogue systems, for a digital system the coverage can no longer be predicted based on signal strength alone. Digital modems are prone to the introduction of an *irreducible* error rate that arises as a result of user motion and/or time dispersion in the channel [1]. The resulting error floors are independent of signal strength and, unless corrected, will eventually limit both the user speed and the maximum data rate that can be supported. Traditionally, the average value of these error floors have been determined either mathematically or through the use of computer simulation.

In this paper the possibility of performing high speed bit error rate *estimation* is investigated through the development of probability density functions based on the instantaneous error rate for a range of fade depths.

It is well known that the RMS delay spread may be used as a good indicator of the time dispersion present in a channel [2]. However, since this value is computed without the use of any fading information, it is difficult to predict the resulting bit error rate. In practice, the average bit error rate is also dependent of the variability

[1] Also President of EDX Engineering, Inc., Eugene, Oregon, U.S.A.

of the local fading envelope. To overcome this problem it is common for the average irreducible bit error rate to be calculated based on Rayleigh fading statistics [3]. For channels experiencing more deterministic, or Ricean-like variations, the average bit error rate will be substantially lower due to the reduced probability of fading.

Since the channel models require sophisticated propagation data, a ray-tracing algorithm is used to generate the required amplitude, time delay, arrival angle and phase information for each received ray. In addition to providing channel models for a full simulation, this ray information can also be used to produce an estimate of the fading statistics in the vicinity of the receiver. This approach improves upon traditional Rayleigh-only channel models since error production can now be achieved for both deterministic and non-deterministic wideband channels.

To improve the speed at which results can be simulated, an importance sampling technique has been developed for *bursty* fading environments. The technique relies on transmitting the data only in locations where there is a reasonable probability or error (i.e. during deep signal fades). For all other locations, the data is assumed to be received correctly, thus greatly reducing simulation run-times.

II - CHANNEL MODEL

A general model of the low-pass impulse response for the mobile transmission channel is shown below:

$$h(t) = \sum_{n=1}^{N} A_n \, \delta \, (\, t - \tau_n \,) \, \exp \, (-j(\theta_n + \Delta\theta_n)) \qquad (1)$$

in which the impulse response $h(t)$ is the sum of a set of N impulses arriving at delay times τ_n with amplitudes A_n, phases θ_n and phase displacements $\Delta\theta_n = 2\pi v t \cos(\varphi_n - \varphi_v)/\lambda$ where φ_n is the arrival angle of the nth impulse, v is the speed of the motion, λ is the carrier wavelength and φ_v is the direction of motion.

To employ this model, it is necessary to identify the amplitudes, time delays and phases of the N constituent components of this response. The components may consist of the directly received signal from the transmitter and a variety of signals received from reflecting surfaces, diffracting corners and scattering surfaces. By
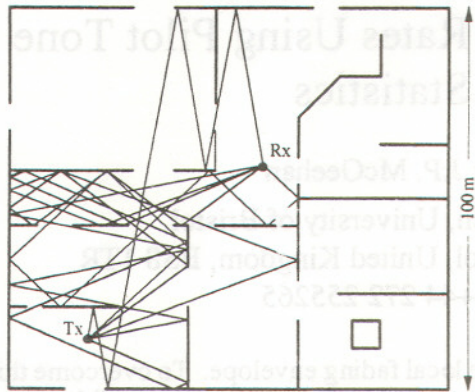
A4.5.1

Figure 1: Typical Output after Ray-Tracing

using a ray-tracing technique, the energy emitted from the source transmitting antenna is geometrically traced to determine those surfaces or corners which are illuminated [4]. For the ray-tracing model used here, each illuminated surface is replaced by an image transmitter or scattering source such that the radiation from the image represents (in amplitude, phase and radiating directions) the energy reflected from the source. Similarly, an illuminated corner is replaced by an equivalent wedge diffraction source. With this first set of images and illuminated corners in place, each of them is then considered in turn by ray-tracing to determine the surfaces and corners they illuminate. Energy from these second reflecting surfaces represent two reflection echoes. This process is repeated for as many iterations as may be relevant to the problem in hand, or which are practical from a computational point of view. Figure 1 shows a typical output from the ray-tracing algorithm. Since this technique inherently provides pulse delay information, it has become attractive for providing the propagation models for digital communication simulations. The ray tracing model is fully described in [5].

At each receive location the ray-tracing propagation model provides three types of information about the channel:

1. Mean signal level (mean channel path loss from the transmitter to the receiver)

2. RMS delay spread and the specific impulse response as define in equation (1)

3. An estimate of the envelope amplitude fading distribution

The mean signal level is found by simply averaging the total power in the rays arriving at the receiver. Fade depth statistics are considered relative to this mean.

The RMS delay spread is the second central moment of the power delay profile with the first arriving ray time τ_{min} referenced as $t=0$. The RMS delay spread is then calculated as below:

$$\sigma_\tau = \left[\sum_{n=1}^{N} (\tau_n - \tau_m)^2 \, p(\tau_n) \right]^{1/2} \quad (2)$$

where the mean value of the power delay profile is:

$$\tau_m = \sum_{n=1}^{N} \tau_n \, p(\tau_n) \quad \text{and} \quad p(\tau_n) = \frac{A_n^2}{\sum_{n=1}^{N} A_n^2} \quad (3)$$

The third channel characteristic which the propagation model provides is an estimate of the probability density function (pdf) for the spatially-dependent envelope amplitude at the receive location. Usually the fading pdf is taken as Rayleigh or lognormally distributed. However, in many receiver locations, especially those which are line-of-sight, the fading pdf is more closely represented by a Ricean distribution. The ray-tracing propagation model provides a means of estimating the actual pdf at a receive location. This is done by supposing that the receiver moves over a number of wavelengths and computing the vector addition of the rays. The resulting set of values is then a sample from the actual fading envelope voltage r, which is a continuous random variable which can be considered stationary in the immediate vicinity of the receive point. Estimates of the the mean $\hat{r}_m$ and variance $\hat{\sigma}_r^2$ of the envelope pdf can be found from the K sample points.

$$\hat{r}_m = \frac{1}{K} \sum_{k=1}^{K} r_k \qquad \hat{\sigma}_r^2 = \frac{1}{K} \sum_{k=1}^{K} (r_k - \hat{r}_m)^2 \quad (4)$$

The general Rice distribution used to represent the envelope amplitude fading distribution is:

$$p(r) = \frac{r}{\sigma_r^2} \exp\left(\frac{-r^2}{2\sigma_r^2}\right) \exp\left(\frac{-A_c^2}{2\sigma_r^2}\right) I_o\left(\frac{rA_c}{\sigma_r^2}\right) \quad (5)$$

where A_c is taken here as the highest amplitude ray in the power delay profile and I_o is the modified Bessel function of the first kind. When A_c is small compared to σ_r, the distribution $p(r)$ is essentially Rayleigh and the fading depth probability follows the well known Rayleigh distribution. When the delay profile is dominated by a single strong ray, the fading envelope distribution is more closely confined around the amplitude of A_c, resulting in less probable fades of a given depth.

The fading envelope distribution $p(r)$ and channel characteristics obtained from the ray-tracing propagation model are then used in conjunction with a system simulation program as explained in the following section.

III - SYSTEM SIMULATION

To allow bit error rates to be determined, a Monte Carlo type simulation was performed with data packets being transmitted until a significant number of errors (or error bursts) had been received. For all results, $\pi/4$ DQPSK has been assumed as the digital modulation scheme.
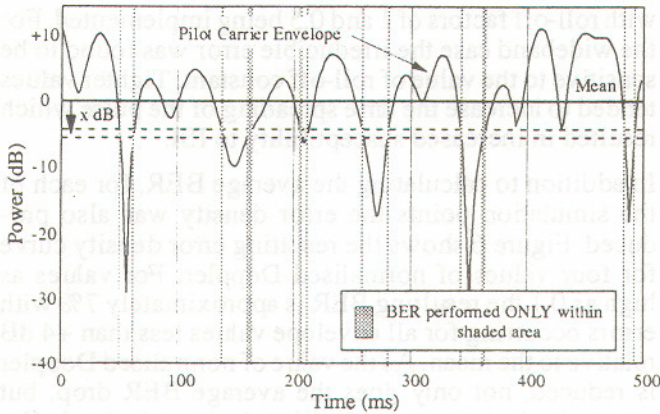
A4.5.2

Figure 2: Error Density Calculation

For each simulation a *pilot* carrier is created which, although not used in the demodulation process, is required to statistically analyse the received waveforms. It is interesting to note that a single tone has been used to sound both the narrowband and the wideband channels. For wideband transmissions the pilot envelope will clearly deviate from the received signal envelope and a more accurate approach may be to generate the fading statistics based on the actual received waveform. This approach has not been implemented since, as will be seen in the next section, it is then more difficult to implement efficient bit error rate *estimation*. In addition, for the relatively low values of delay spread investigated (compared to the bit rate), the narrowband envelope provides an excellent indicator of system error.

It is well known that the errors introduced by factors such as random FM and time dispersion occur in bursts and that these bursts are highly correlated with fade depth (at least for low values of error). To investigate this relationship, a probability density function was constructed based on the pilot fading information and the resulting BER. The pilot signal is first analysed to determine its mean value. The envelope is then divided into thin sections as demonstrated in figure 2. The diagram shows a typical 1 dB segment that is offset by x dB from the mean (x varied from +15 to -40 dB). The resulting bit error rate is then calculated for all the data bits for which the pilot envelope falls within this range of values (i.e. the shaded regions in figure 2). This process produces an average bit error rate at regular offsets from the mean and can be used to demonstrate the bursty nature of the mobile channel.

The average bit error rate for a given location can be computed using equation 6, where $p(r)$ represents the pdf of the fading envelope and $e(r)$ the error density function calculated above.

$$\text{BER} = \int_{-\infty}^{+\infty} p(r)e(r)\, dr \approx \sum_{r=-40}^{+15} p(r)e(r) \qquad (6)$$

Hence, by combining the fading pdf estimate for a given location with the error density results obtained above, it becomes possible to obtain high speed estimations for the average bit error rate in a given location. In addition some appreciation of the instantaneous bit error rate can also be produced based on knowledge of the signal envelope relative to the mean. However, for certain applications a more thorough examination may be necessary and this requires the implementation of a full simulation.

IV - IMPORTANCE SAMPLING

Monte Carlo simulations generally require extremely large run times to confidently predict low values of bit error rate. Traditionally, a minimum of around 100-200 bit errors are received for each point in the simulation. For an error rate of 1E-5, this requires the transmission of approximately 10-20 million bits. For a bursty environment the above criteria is questionable since all the errors could occur in a single burst. Ideally, for a fading environment, the resulting bit error rate should be averaged over a large number of these error bursts.

In traditional simulations, a great deal of run time can be wasted by simulating transmission in areas where the probability of bit error is low. With this in mind, an alternative approach has been implemented that simulates data transmission *only* during fades. Figure 3 demonstrates the principals behind this technique. A narrowband pilot tone is first passed though the fading model to generate a large sample of the fading waveform. The resulting envelope is then analysed using a pre-determined value to determine the points at which the signal falls below (τ_{ak}) and above (τ_{bk}) this threshold. The resulting data table, which stores the time for all the relevant fades, can now be used by the main simulation to prevent run-time being wasted in those areas where error is unlikely to occur.

The threshold is obviously critical to the success of this approach and can be determined from the bit error probability density functions described earlier. In practice, for very low error rates, to generate an error the signal may need to fade in excess of 20 dB relative to the mean. For this type of situation, the run time could be improved by as much as two orders of magnitude. The improvement factor (R) is given by equation 7,
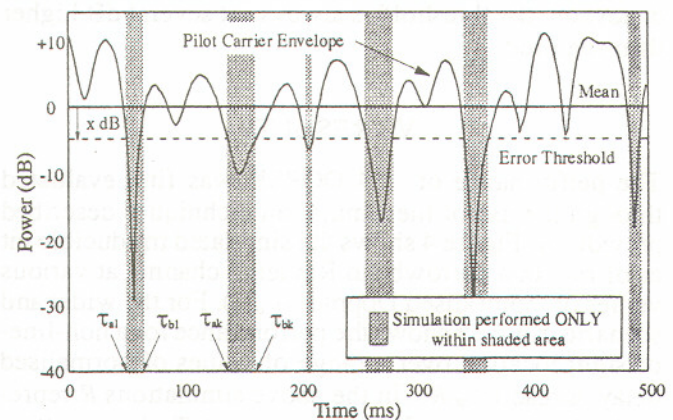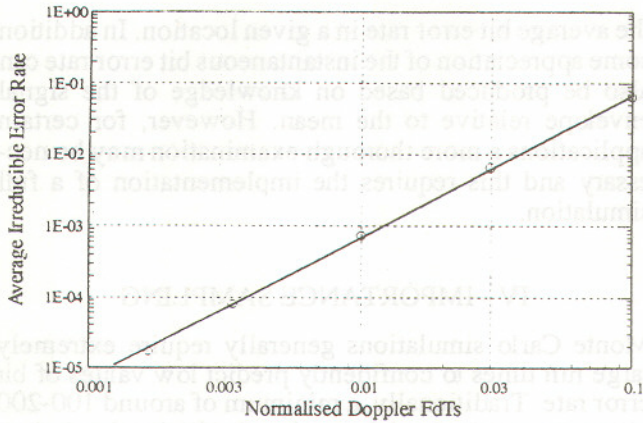

Figure 3: Error Density Calculation

Figure 4: Irreducible BER vs. Normalised Doppler
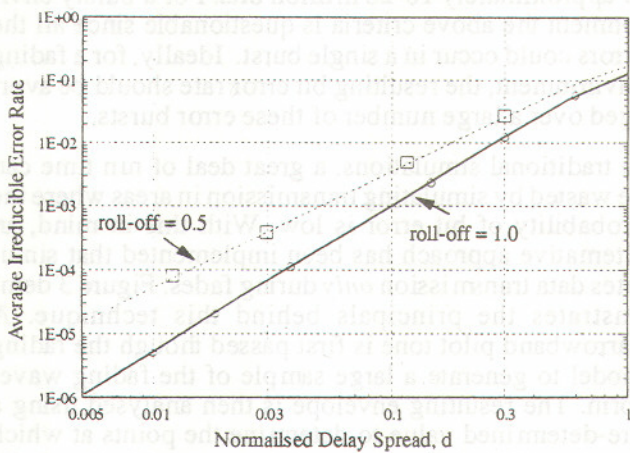

Figure 5: Irreducible BER vs. Normalised Delay

where $P(r<x)$ represents the Rayleigh cumulative pdf and x the pre-determined threshold.

$$R = \frac{1}{P(r<x)} \qquad (7)$$

From equation 7 it is obviously that as the threshold is lowered, the overall improvement increases. However, it is important to note that if, for a particular run, the threshold is set too low, invalid error rates will be generated. In practice, to minimise the probability of distortion, the threshold is always set several dB higher than required.

V - RESULTS

The performance of $\pi/4$ DQPSK was first evaluated through the use of the simulation techniques described previously. Figure 4 shows the simulated irreducible bit error rate in a narrowband Rayleigh channel at various values of normalised Doppler (F_dT_s). For the wideband scenario, figure 5 shows the performance for a non-line-of-sight location over a range of values of normalised delay spread ($\tau_{RMS}R$). In the above simulations R represents the bit rate of the system and T_s the resulting symbol period. Root raised cosine filtering was assumed

with roll-off factors of 1 and 0.5 being implemented. For the wideband case the irreducible error was found to be sensitive to the value of roll-off constant. Tighter values tended to increase the time spreading of the pulse which resulted in increased susceptibility to ISI.

In addition to calculating the average BER, for each of the simulation points the error density was also produced. Figure 6 shows the resulting error density curve for four values of normalised Doppler. For values as high as 0.1 the resulting BER is approximately 7% with errors occurring for all envelope values less than +4 dB relative to the mean. As the value of normalised Doppler is reduced, not only does the average BER drop, but errors also become more correlated with fade depth. For a normalised Doppler of 0.003, the signal envelope had to fade grater than -25 dB relative to the mean before errors were likely to occur. This burst phenomenon occurs since the rate of change of phase is directly proportional to the depth of the fade. Indeed, at the bottom of extreme fades (>-40dB), the resultant phasor
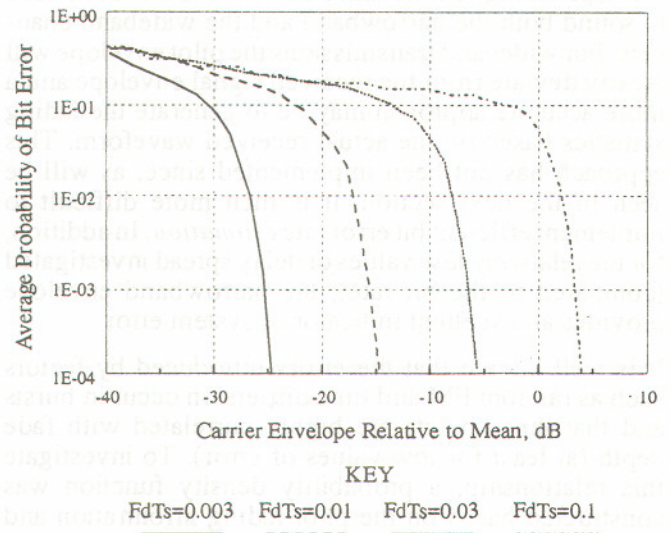

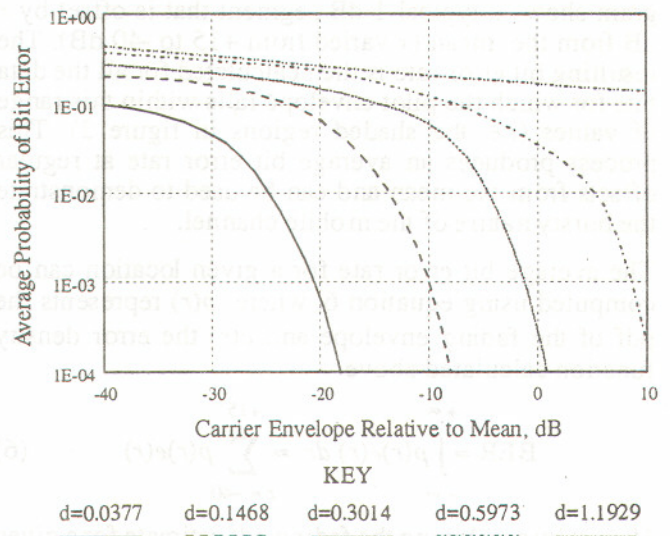Figure 6: Error Density for Random FM (Doppler)

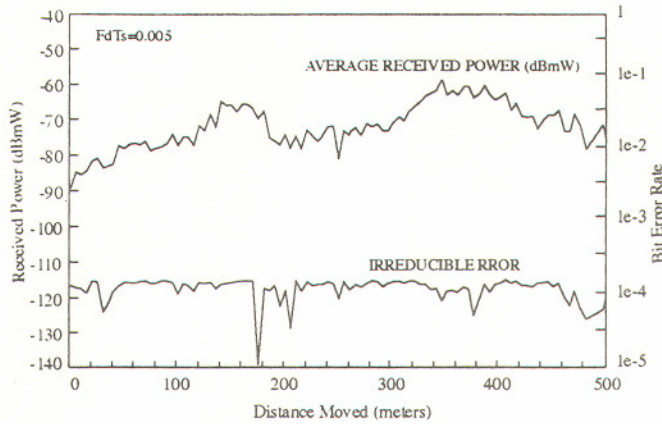Figure 7: Error Density in Normalised Delay Spread
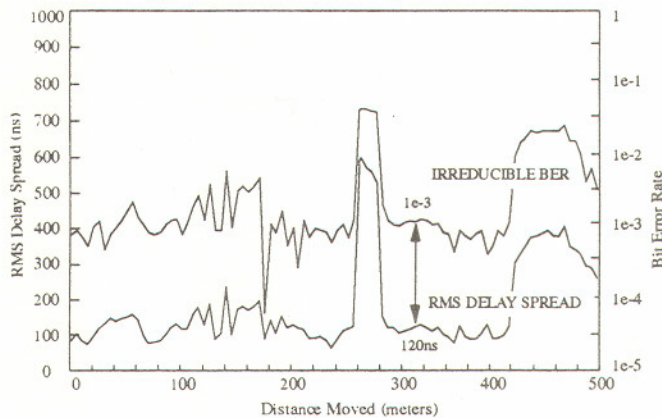
Figure 8: Error Density Calculation

Figure 9: Error Density Calculation

can flip by up to 180 degrees thus introducing highly correlated errors.

A similar phenomenon also occurs for the wideband situation. Figure 7 shows the correlation between the bit error rate and the instantaneous fade depth.

The degree of frequency selective fading is determined by the normalised delay spread. For low values of d (~0.0377), the errors tend to be restricted to deep signal fades (greater than 20 dB relative to the mean). From figure 5 it can be seen that the average bit rate in this region is approximately 1E-4 (assuming a roll-off of 1), however, during deep signal fades the instantaneous bit error rate can be significantly higher. Values greater than 1 in 100 are possible for fade depths greater than 25 dB. This illustrates one of the problems of using an average bit error rate for a bursty channel. As either the normalised delay spread or the normalised Doppler increases, the correlation between the average bit error rate and the signal envelope reduces. For a normalised delay spread of 0.3014, bit errors can occur whenever the pilot fades below its mean (i.e. approximately 50% of locations). As the delay spread is further increased, bit errors occur for all values of pilot envelope. For delay spread greater than 1.2 almost no correlation was measured between the pilot envelope and the instantaneous bit error rate.

From figures 6 and 7 it can be seen that as the average BER falls, the resulting errors become highly correlated

with fade depth. It therefore follows that simulating transmission in high signal strengths results in no useful information. To reduce the time required to obtain data points in this region, the speed-up technique described in section IV was applied. A threshold of -15 dB was used and this resulted in an approximate thirty times reduction in run-time. Indeed, this technique was applied to obtain the very low error rates shown in figure 5, where traditionally up to 50 million data bits would have needed to be transmitted. However, the resulting BER is now very sensitive to the tail of the fading pdf. A great deal of care must therefore be taken to generate channel models which accurately represents this region.

The aim of this work is to allow accurate estimates for the average irreducible BER to be determined without the need for simulation. In addition, since the average bit error rate depends on the degree of envelope fading, the technique should also make use of localised fading information.

To demonstrate this technique, the receiver was moved at a given speed within the ray-tracing program. For each location the propagation characteristics were evaluated and, based on user's speed, carrier frequency and data rate, appropriate pdf's generated for random FM and delay spread (through interpolation of the results shown in figures 6 and 7). This information was then inserted into equation 6 where a discrete summation was performed to obtain estimates for the average irreducible bit error rates. If required, a similar summation can also be performed based on the AWGN performance of the chosen modulation scheme. The error rates for AWGN, e_n, random FM, e_r and RMS delay spread, e_D, are then combined as shown below:

$$\text{Average BER} = (e_n^2 + e_r^2 + e_D^2)^{1/2} \qquad (8)$$

The output from equation 8 then represents the desired estimate for the overall average BER. Figure 8 shows a plot of the irreducible error resulting from random FM as the receiver moves along its pre-determined route. A normalised Doppler value of 0.005 (62 kb/s, 100 km/h, 1.8 GHz) was assumed which, from figure 8, resulted in a maximum error floor of nearly 2E-4 (depending on fading statistics). From figure 4, assuming a Rayleigh envelope distribution, an error floor of 2E-4 was obtained through simulation.

Figure 9 shows a similar result for normalised delay spread. For a value of 120 ns, an error floor of 1E-3 is predicted. Using figure 7, the value obtained through simulation was approximately 1.5E-3 (d=0.12). More importantly, the estimated average BER is now a function of not only the RMS delay spread, but also the propagation characteristics of the local environment.

VI- CONCLUSIONS

An error rate estimation technique has been developed which uses narrowband envelope fading statistics to predict irreducible error rates. It has been shown that the BER in a channel is related to the local fading pdf and

this information has been included in the generation of our estimates. An accelerated simulation technique has been developed and shown to be particularly useful for evaluating the extremely low error rates that occur as a result of deep and infrequent fading.

REFERENCES

[1] A.R. Nix, G.H. Norton, J.P. McGeehan, "Error Rate Analysis for Indoor Wireless Networks", 42nd IEEE VTS Conf., Denver, USA, 11-13 May 1992, pp 808-813.

[2] F. Adachi, K. Ohno, "BER Performance of QDPSK with Postdetection Diversity Reception in Mobile Radio Channels", IEEE Trans. on Veh. Tech., Vol. 40, No. 1, Feb 1991, pp 237-249.

[3] Y.C. Chow, A.R.Nix, J.P McGeehan,"Analysis of 16-APSK Modulation in AWGN and Rayleigh Fading Channels", IEE Electronic Letters, 13th August 1992, Vol. 28, No. 17, pp1608-1610.

[4] M.C. Lawton, R.L Davies, J.P. McGeehan, "An Analytical Model for Indoor Multipath Propagation in the Picocellular Environmnet", 42nd IEEE VTS Conf., Denver, USA, 11-13 May 1992, pp 808-813.

[5] H.R. Anderson, A.R.Nix, J.P McGeehan,"Theoretical Polarization Diversity Studies in an Urban Microcell Environment", 4th Int. Sym. on Personal and Mobile Radio communications, 8-11 Sept. 1993